



Title	Magnetic field dependence of threshold electric field for magnetoelectric switching of exchange-bias polarity
Author(s)	Nguyen, Thi Van Anh; Shiratsuchi, Yu; Kobane, Atsushi et al.
Citation	Journal of Applied Physics. 2017, 122(7), p. 073905
Version Type	VoR
URL	https://hdl.handle.net/11094/89973
rights	This article may be downloaded for personal use only. Any other use requires prior permission of the author and AIP Publishing. This article appeared in Thi Van Anh Nguyen, Yu Shiratsuchi, Atsushi Kobane, Saori Yoshida, and Ryoichi Nakatani, Journal of Applied Physics 122, 073905 (2017) and may be found at https://doi.org/10.1063/1.4991053 .
Note	

The University of Osaka Institutional Knowledge Archive : OUKA

<https://ir.library.osaka-u.ac.jp/>

The University of Osaka

Magnetic field dependence of threshold electric field for magnetoelectric switching of exchange-bias polarity

Cite as: J. Appl. Phys. **122**, 073905 (2017); <https://doi.org/10.1063/1.4991053>

Submitted: 19 June 2017 • Accepted: 30 July 2017 • Published Online: 17 August 2017

Thi Van Anh Nguyen, Yu Shiratsuchi, Atsushi Kobane, et al.



View Online



Export Citation



CrossMark

ARTICLES YOU MAY BE INTERESTED IN

[Magnetoelectric switching of perpendicular exchange bias in Pt/Co/ \$\alpha\$ -Cr₂O₃/Pt stacked films](#)

Applied Physics Letters **106**, 162404 (2015); <https://doi.org/10.1063/1.4918940>

[Energy condition of isothermal magnetoelectric switching of perpendicular exchange bias in Pt/Co/Au/Cr₂O₃/Pt stacked film](#)

Journal of Applied Physics **124**, 233902 (2018); <https://doi.org/10.1063/1.5047563>

[Simultaneous achievement of high perpendicular exchange bias and low coercivity by controlling ferromagnetic/antiferromagnetic interfacial magnetic anisotropy](#)

Journal of Applied Physics **121**, 073902 (2017); <https://doi.org/10.1063/1.4976568>

Journal of
Applied Physics

Special Topics Open for Submissions

Learn More

Magnetic field dependence of threshold electric field for magnetoelectric switching of exchange-bias polarity

Thi Van Anh Nguyen, Yu Shiratsuchi,^{a)} Atsushi Kobane, Saori Yoshida, and Ryoichi Nakatani

Department of Materials Science and Engineering, Graduate School of Engineering, Osaka University, 2-1 Yamadaoka, Suita, Osaka 565-0871, Japan

(Received 19 June 2017; accepted 30 July 2017; published online 17 August 2017)

We report the magnetic field dependence of the threshold electric field E_{th} for the magnetoelectric switching of the perpendicular exchange bias in Pt/Co/Au/Cr₂O₃/Pt stacked films using a reversible isothermal electric tuning approach. The E_{th} values for the positive-to-negative and negative-to-positive switching are different because of the unidirectional nature of the interfacial exchange coupling. The E_{th} values are inversely proportional to the magnetic-field strength, and the quantitative analysis of this relationship suggests that the switching is driven by the nucleation and growth of the antiferromagnetic domain. We also find that the magnetic-field dependence of E_{th} exhibits an offset electric field that might be related to the uncompensated antiferromagnetic moments located mainly at the interface. *Published by AIP Publishing.* [<http://dx.doi.org/10.1063/1.4991053>]

I. INTRODUCTION

Recently, the electric field control of perpendicular magnetization based on magnetoelectric (ME) insulator films has been receiving much interest for the realization of advanced spintronic devices with superior advantages such as high integration, high processing speed, and low power consumption.^{1–7} Antiferromagnetic (AFM) Cr₂O₃, which is a type of ME insulator, generates a perpendicular exchange bias (EB) when coupled with a ferromagnetic (FM) layer.^{7,8} Owing to the unidirectional nature of exchange coupling at the FM/AFM interface, the EB manifests itself through a shift of the magnetic hysteresis loop of the FM layer, away from the zero magnetic field.^{9–11} Especially, when the EB field exceeds the coercivity of the FM layer, the magnetization direction of the FM layer at a remanent state can be defined to be of one particular direction.

The electric control of the EB polarity using the ME effect of Cr₂O₃ has been an area of active pursuit.^{2–5,7,8,12} Previously, in bulk systems, the electric-field-induced tuning of the EB polarity was achieved in an isothermal manner.^{2–5} Recently, an all-thin-film system was reported in which reversible isothermal switching occurred with the change in the EB polarity from negative to positive (N-to-P process) and vice versa (P-to-N process), by tuning the applied electric field E while maintaining the magnetic field H .⁵ However, more details on the energy conditions for ME switching, which are important from both the application and fundamental points of view, were not reported. One approach is to demonstrate the relationships between the applied E and H and the ME switching conditions in the system; these were partially revealed in our previous paper.^{4,7} The threshold electric field E_{th} at which the EB polarity is reversed depends on the H , and the energy condition is roughly suggested to follow a linear relationship, $EH = \text{constant}$.^{2,4,7,13} Nevertheless, a

study on the magnetic-field dependence of E_{th} , in a reversible manner, has not been conducted satisfactorily yet. In this paper, we present a systematic study on the magnetic field dependence of E_{th} for the ME switching of the perpendicular EB in a Pt/Co/Au/Cr₂O₃/Pt system using a reversible isothermal electric tuning approach. The ME switching energy conditions are studied further under different magnetic-field-cooling (FC) conditions in order to explore the intrinsic behavior of ME switching.

II. EXPERIMENTAL METHODS

The Pt(1.2)/Co(0.4, 0.6)/Au(0.5)/Cr₂O₃(150, 200)/Pt(20) stacked films were prepared on α -Al₂O₃(0001) substrates through DC magnetron sputtering. The numbers in the parentheses denote the thickness of each layer, in nanometers. The base pressure of the sputtering chamber was maintained below 10^{-6} Pa. First, the Pt(111) buffer layer was deposited on the α -Al₂O₃(0001) substrate at room temperature (RT) and was annealed for 1 h at 873 K. Then, the Cr₂O₃(0001) layer was deposited on the Pt(111) buffer layer at 773 K under a flow of mixed argon and oxygen. The Au spacer, the FM Co layer, and the Pt capping layer were deposited at RT under argon gas flow. The Au layer between Co and Cr₂O₃ layers was used to control the interface exchange coupling energy, which is necessary, so that the exchange bias persists up to the high temperature regime in which the ME control of the exchange bias is accessible. The Au spacer layer is also effective in getting perpendicular interfacial spins which result in both a high exchange bias field and low coercivity in the sample.¹⁴ The structural characterization was done using *in-situ* reflection high-energy electron diffraction (RHEED) and X-ray diffraction. The magnetic properties were analyzed using vibrating sample magnetometry and magneto-optic Kerr effect magnetometry. More details on sample preparation and structural and magnetic characterization can be found in our previous paper.¹⁴

^{a)}Author to whom correspondence should be addressed: shiratsuchi@mat.eng.osaka-u.ac.jp

The isothermal switching of EB polarity was investigated by conducting anomalous Hall effect (AHE) measurements on a microfabricated Hall device of width $2\ \mu\text{m}$ and length $40\ \mu\text{m}$, fabricated by photolithography, Ar ion-milling techniques, and lift-off processes. The optical microscopy image of the fabricated device along with the measurement setups is shown in Fig. 1. In our device, the electric field was varied by changing the bias voltage applied across the $\text{Cr}_2\text{O}_3(0001)$ layer between the top electrode (Pt cap layer) and the bottom electrode (Pt buffer layer). The magnetic field was applied in a direction perpendicular to the surface normal. The positive direction of the field was defined as the direction from the bottom electrode to the top electrode of the device. The energy condition for ME switching was studied after an FC process from 310 K to the measurement temperature, under different cooling fields of $-6\ \text{kOe}$, $+6\ \text{kOe}$, and $+10\ \text{kOe}$. The ME switching was measured at 275–285 K by changing E from $-733\ \text{kV/cm}$ to $+750\ \text{kV/cm}$, while keeping the H field at one of these values: $+60\ \text{kOe}$, $+50\ \text{kOe}$, $+45\ \text{kOe}$, $+40\ \text{kOe}$, $-40\ \text{kOe}$, $-45\ \text{kOe}$, $-50\ \text{kOe}$, $-55\ \text{kOe}$, or $-60\ \text{kOe}$. To check the EB polarity after the abovementioned simultaneous application of both E and H , the AHE loops were measured as functions of the perpendicular magnetic field in the range of $\pm 1.5\ \text{kOe}$. During AHE measurements, the electric field was set to $0\ \text{kV/cm}$.

III. RESULTS AND DISCUSSION

First, we show that the EB polarity is reversibly switched in an isothermal manner at 280 K, by varying E under a constant magnetic field $H = +60\ \text{kOe}$ [Fig. 2(a)] for the $\text{Pt}(1.2)/\text{Co}(0.4)/\text{Au}(0.5)/\text{Cr}_2\text{O}_3(150)/\text{Pt}(20)$ stacked film. The initial state is defined after the FC process under $-6\ \text{kOe}$, and thus, the EB is initially defined in a positive direction (gray open circle). Starting from this positive EB state, the EB polarity is switched to negative after applying $E = -467\ \text{kV/cm}$ (blue closed circle). Then, from this negative EB state, the EB polarity is switched again, to positive, by applying $E = +333\ \text{kV/cm}$ (red open square). The intermediate state, i.e., the partially switched state is also observed, for example, in the case of $E = -400\ \text{kV/cm}$ (green closed triangle). In the intermediate state, the two loops with negative and positive EBs are superimposed, indicating that the reversed and unreversed regions coexist. In an AHE

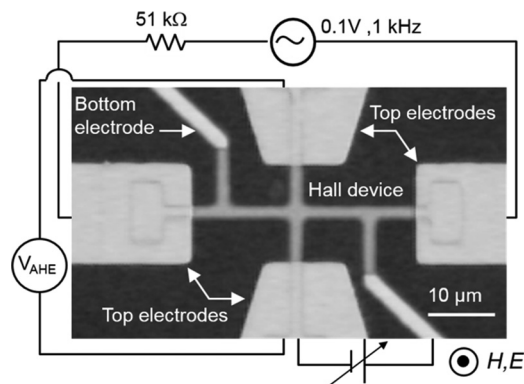


FIG. 1. Optical microscopy image of the Hall device with the anomalous Hall effect (AHE) measurement setup.

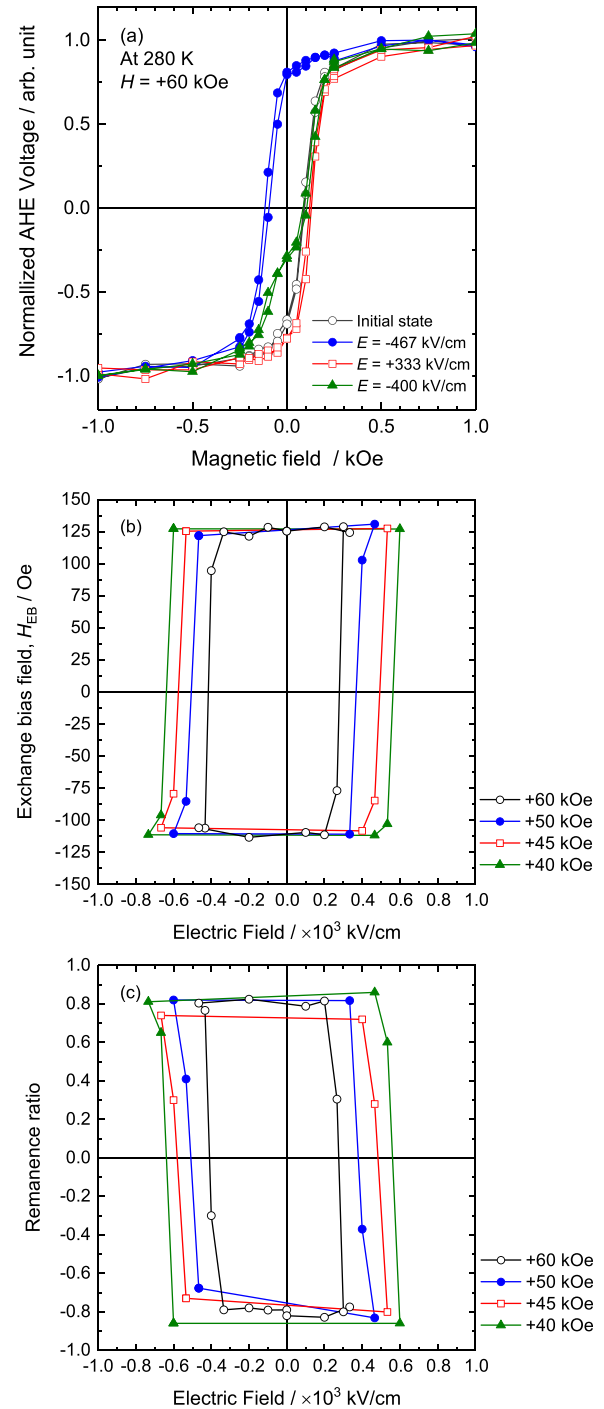


FIG. 2. (a) Typical ME switching of the exchange bias (EB) field under the magnetic field of $+60\ \text{kOe}$ at 280 K. The hysteretic electric field dependence of (b) EB field and (c) remanence ratio. All data were collected after a similar initial field cooling process under $-6\ \text{kOe}$, more details are given in the main text.

loop, in addition to the change in the EB polarity, the remanence ratio reflecting the ratio of the two regions is also appropriate for evaluating the switching condition. Therefore, both values of the EB field H_{EB} and the remanence ratio $M_{\text{R}}/M_{\text{S}}$ can be evaluated as functions of E , as shown in Figs. 2(b) and 2(c), respectively. To collect each data point, the device is initialized to the fully positive-EB (or negative-EB) state by applying $E = +333\ \text{kV/cm}$ (or $-467\ \text{kV/cm}$) for the P-to-N (or N-to-P) switching process.

The rectangular hysteresis is in agreement with the isothermal switching of the AFM domain state in Cr_2O_3 .¹³ Similar behaviors are obtained at different constants H , i.e., $H = +50$ kOe, $+45$ kOe, and $+40$ kOe [Figs. 2(b) and 2(c)]. From the hysteresis loop of M_R/M_S [Fig. 2(c)], the E_{th} values for both the P-to-N and N-to-P processes are estimated from the intersecting point of the loop with the horizontal axis, at which M_R/M_S changes the sign. The asymmetry of the E_{th} values between the N-to-P and P-to-N processes is attributed to the unidirectional nature of exchange coupling at the FM/AFM interface.

In order to assess the energy conditions of ME switching, we investigate the change in E_{th} for a constant H strength. In Fig. 3, the changes in E_{th} are shown as functions of $1/H$, for both P-to-N (blue circle) and N-to-P switching (blue square). E_{th} is inversely proportional to H , meaning that the EH product is constant under the threshold conditions. This is simply interpreted as: the energy gain by the ME effect is expressed by αEH , where α is an ME coefficient.^{13,15} To examine the ME switching conditions in more detail, we show the magnetic-field dependence of E_{th} under different FC conditions: $+6$ kOe (green circle and square) and $+10$ kOe (black circles and square) in Fig. 3. The $E_{\text{th}}-1/H$ curves for different cooling fields show that E_{th} is independent of both the cooling-field strength and the cooling-field direction, under the studied conditions. In other systems, it was reported that the H_{EB} altered with the change in the cooling field; it was associated with the difference in the crystalline orientations of the AFM,¹⁶ or the coupling between the interfacial spins of the AFM layer with the external cooling field.^{17,18} In our research, the independence of the $E_{\text{th}}-1/H$ relationship from the cooling conditions implies the stability of the interfacial spin structure under the studied conditions.

In the previous report,⁴ the energy conditions for ME switching were assumed to follow the coherent rotation

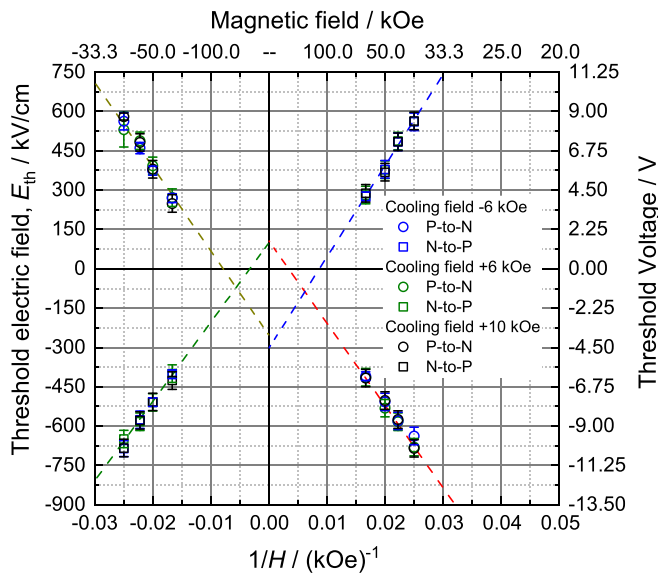


FIG. 3. Magnetic field dependence of the threshold electric field for switching EB polarity for both P-to-N and N-to-P processes, under different cooling fields of -6 kOe (blue marks), $+6$ kOe (red marks), and $+10$ kOe (black marks). The dashed lines are the guides to evaluate E_0 .

model, in which the ME effect led to an energy gain for switching the EB polarity. Under the application of external electric and magnetic fields, the total energy per unit area, including the magnetic anisotropy energy density K_{AFM} , the Zeeman energy, and the interfacial exchange coupling energy density J , is expressed as

$$F = K_{\text{AFM}} t_{\text{AFM}} \sin^2 \theta - \alpha_{33} E H t_{\text{AFM}} \cos \theta - J S_{\text{FM}} S_{\text{AFM}} \cos \theta, \quad (1)$$

where t_{AFM} is the thickness of the AFM layer, α_{33} is the ME coefficient along the c axis of Cr_2O_3 , S_{FM} and S_{AFM} are the interfacial FM and AFM spins, and θ is the angle between the interfacial AFM and FM spins. Because the constant magnetic field H was sufficiently higher than the saturation field of FM magnetization, θ can also be interpreted as the angle between the AFM spins and H . In the $E_{\text{th}}-1/H$ curves shown in Fig. 3, it can be observed that there is a shift in the E_{th} intercept from the origin. As discussed below, this shift can be caused by the finite uncompensated antiferromagnetic moment, M_{AFM} , which is located at both the bulk site and the interface. As the M_{AFM} at the bulk site,¹⁹ the pure magnetic switching of the interfacial M_{AFM} ^{20,21} and the resultant isothermal switching of the exchange polarity²² via the Zeeman energy are also possible. Hence, the Zeeman term of M_{AFM} is reasonable to be considered and the Zeeman energy term for M_{AFM} was added to Eq. (1), and then,

$$F = K_{\text{AFM}} t_{\text{AFM}} \sin^2 \theta - \alpha_{33} E H t_{\text{AFM}} \cos \theta - J S_{\text{FM}} S_{\text{AFM}} \cos \theta - M_{\text{AFM}} H \cos \theta = K_{\text{AFM}} t_{\text{AFM}} \sin^2 \theta - (\alpha_{33} E t_{\text{AFM}} + M_{\text{AFM}}) H \cos \theta - J S_{\text{FM}} S_{\text{AFM}} \cos \theta. \quad (1a)$$

The switching condition was derived from Eq. (1a) by minimizing the total energy per unit area. Namely,

$$\frac{\partial F}{\partial \theta} = 0, \quad \frac{\partial^2 F}{\partial \theta^2} > 0. \quad (2)$$

The solution can be obtained for two different initial states, i.e., $\theta = 0$ or π . For each case, the energy condition can be simply expressed as

$$\left(\alpha_{33} E + \frac{M_{\text{AFM}}}{t_{\text{AFM}}} \right) H = -2K_{\text{AFM}} - \frac{J S_{\text{FM}} S_{\text{AFM}}}{t_{\text{AFM}}} \quad \text{for P-to-N switching,} \quad (3-1)$$

$$\left(\alpha_{33} E + \frac{M_{\text{AFM}}}{t_{\text{AFM}}} \right) H = 2K_{\text{AFM}} - \frac{J S_{\text{FM}} S_{\text{AFM}}}{t_{\text{AFM}}} \quad \text{for N-to-P switching.} \quad (3-2)$$

Considering that the parameters in Eqs. (3-1) and (3-2) are constant as long as the temperature is maintained, Eqs. (3-1) and (3-2) suggest that the $E_{\text{th}}-1/H$ relationship should be linear. In addition, Eqs. (3-1) and (3-2) also suggest that the average and difference of the slopes of the $E_{\text{th}}-1/H$ curves yield $K_{\text{AFM}}/\alpha_{33}$ and $J S_{\text{FM}} S_{\text{AFM}}/(t_{\text{AFM}} \alpha_{33})$, respectively. From the results in Fig. 3, these values are estimated

as $K_{\text{AFM}} = 4.5 \pm 0.6 \times 10^4 \text{ erg/cc}$ and $JS_{\text{FM}}S_{\text{AFM}} = 1.5 \pm 0.2 \times 10^{-2} \text{ erg/cm}^2$, respectively, assuming $\alpha_{33} = 3\text{--}4 \text{ ps/m}$ at 280 K (Refs. 15, 19, 23, and 24) as the value for bulk and 500 nm thick Cr_2O_3 thin films. The estimated K_{AFM} value is approximately half of the K_{AFM} of bulk Cr_2O_3 at 280 K, $\sim 1 \times 10^5 \text{ erg/cc}$,²⁵ and this is probably because the above equations assume coherent rotation, whereas, in actual, the reversals proceed via the reversed AFM spin/domain nucleation and growth. We can observe the multidomain state and the expansion of the reversed domain region with increasing E .²⁶

$JS_{\text{FM}}S_{\text{AFM}}$ can be compared with the exchange anisotropy energy density $J_K = H_{\text{EB}}M_S t_{\text{FM}}$, where M_S is the saturation magnetization of the FM layer and t_{FM} is the FM layer thickness; $JS_{\text{FM}}S_{\text{AFM}}$ corresponds to J_K in the pinned spin model.^{9–11} Using the experimentally obtained H_{EB} and M_S values, J_K at 280 K is estimated as $\sim 5.8 \times 10^{-3} \text{ erg/cm}^2$, which is approximately one-third of the above estimated $JS_{\text{FM}}S_{\text{AFM}}$ value, which is in agreement with the well-known fact that the pinned spin model overestimates the exchange anisotropy energy density.^{9–11} This is also consistent with our previous paper²⁷ in which we showed that the interfacial uncompensated AFM (Cr) spins were not pinned but could reverse together with the FM spin reversal; the pinned spin model is not valid for our film.

Finally, we discuss the shift of the E_{th} intercept from the origin, E_0 in the $E_{\text{th}}\text{--}1/H$ curves. According to Eqs. (3-1) and (3-2), E_0 should be proportional to $M_{\text{AFM}}/t_{\text{AFM}}$. Recently, Kosub *et al.* attributed M_{AFM} to the defect-induced uncompensated AFM moment (emergent ferrimagnet) coupled with the AFM order parameter.¹² In our study, since the ME switching was detected through the exchange bias, M_{AFM} should be considered as the AFM moments exchange-coupled with the FM spins. As long as the exchange bias is induced by the interfacial exchange coupling at the FM/ Cr_2O_3 interface, it is reasonable to assume that the interfacial M_{AFM} should have a significant role in E_0 . According to our previous paper, the interfacial uncompensated Cr spins are antiferromagnetically coupled with the FM spins. Supposing the N-to-P switching for the positive magnetic field (blue dotted line in Fig. 3), the interfacial M_{AFM} are antiparallel to H (and FM spins) and E , and thus, $\alpha_{33}E$ and M_{AFM} are antiparallel. Consequently, the $E_{\text{th}}\text{--}1/H$ curves shift toward negative, consistent with the experimental results.

From Fig. 3, one can find that there exists the following relationship:

$$\begin{aligned} E_0(\text{N-to-P}, H > 0) &\approx E_0(\text{P-to-N}, H < 0), \\ E_0(\text{P-to-N}, H > 0) &\approx E_0(\text{N-to-P}, H < 0). \end{aligned} \quad (4)$$

E_0 for each case can be estimated as $-300 \pm 20 \text{ kV/cm}$ or $+100 \pm 5 \text{ kV/cm}$, depending on the sign of the constant H field; E_0 is positive (negative) when the EB switches toward (against) the constant magnetic-field direction. According to Eqs. (3-1) and (3-2), the asymmetry of E_0 implies that there is a difference in M_{AFM} for the P-to-N and N-to-P switching. When the M_{AFM} are fully reversed in our exchange-biased system, E_0 would become symmetric, i.e., the absolute values of E_0 are similar for the N-to-P and P-to-N switching. In

the previous report,²⁷ we reported that the difference in M_{AFM} and the asymmetric spin alignment with respect to the magnetic-field direction were present at the interface uncompensated AFM moments using the element-specific magnetization curve (ESMC) of Cr in the Pt/Co/ Cr_2O_3 /Pt exchange-biased film: the vertical shift of the ESMC curve of Cr. The vertical shift of ESMC causes the difference in M_{AFM} for N-to-P and P-to-N switching, and consequently, E_0 becomes asymmetric. The direction of the vertical shift coupled with the polarity of the exchange bias, and among the absolute values of X-ray magnetic circular dichroism (XMCD) intensity, one could find the following relationship [see Fig. 3(b) of Ref. 27]

$$\begin{aligned} |M_{\text{AFM}}(\text{N-to-P}, H > 0)| &\approx |M_{\text{AFM}}(\text{P-to-N}, H < 0)| \\ |M_{\text{AFM}}(\text{P-to-N}, H > 0)| &\approx |M_{\text{AFM}}(\text{N-to-P}, H < 0)|. \end{aligned} \quad (5)$$

This similarity of the absolute value is consistent with the similar absolute value of E_0 , i.e., the relationship shown in Eq. (4).

While in the above discussion, we focused on the interfacial uncompensated AFM moments, the defect-induced uncompensated AFM moment or the emergent ferrimagnet at the bulk site can also affect the interfacial AFM moments via the AFM order parameter. However, the existence of the emergent ferrimagnetism in our Cr_2O_3 film has to be investigated in more detail because no XMCD signal was observed in the Pt/ Cr_2O_3 /Pt/Ta/SiN membrane for both the surface-sensitive total electron yield method and the bulk-sensitive transmission methods in our previous paper.²⁸

As long as M_{AFM} couples with the AFM order parameter, M_{AFM} and E_0 depend on temperature. As shown in Fig. 4, the absolute value of E_0 increases with decreasing temperature except at 275 K for the N-to-P switching. The temperature dependence of E_0 may reflect that of M_{AFM} ,

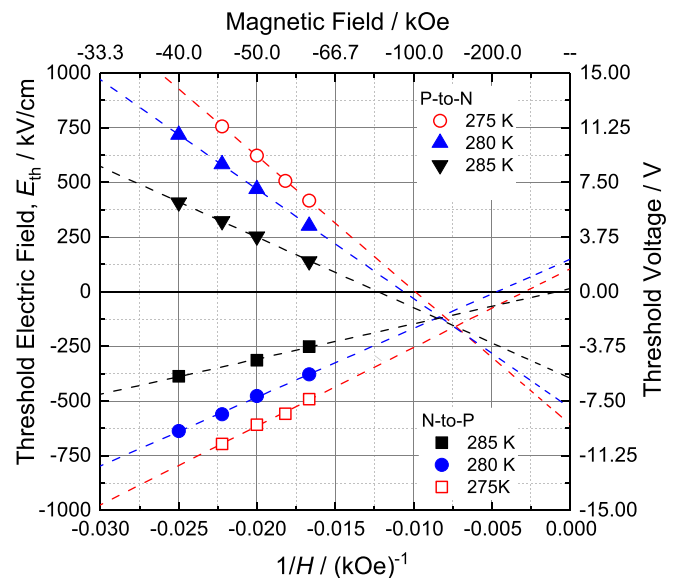


FIG. 4. $E_{\text{th}}\text{--}1/H$ curves at different temperatures of 275, 280, and 285 K for the Pt(1.2)/Co(0.6)/Au(0.5)/ Cr_2O_3 (200)/Pt(20) stacked film. The dashed lines are the guides to evaluate E_0 .

but it is a nontrivial problem. As mentioned above, both interface and bulk uncompensated AFM moments contribute to M_{AFM} , and these two can exhibit the different temperature dependence. Especially, the interface uncompensated AFM moments which should be the origin of the asymmetry of E_0 can possess a different critical exponent β from that of the AFM order parameter.²⁹ Hence, the symmetric and asymmetric contributions to E_0 can exhibit a different temperature dependence. In order to arrive at a definite conclusion for the temperature dependence of E_0 , much more data points are necessary and further investigations are needed.

IV. SUMMARY

The magnetic-field dependence of E_{th} for the ME switching of perpendicular EB in a reversible isothermal electric tuning approach was investigated. The E_{th} was found to be inversely proportional to the magnetic field, agreeing with the ME-induced mechanism. The E_{th} values were different for P-to-N and N-to-P switching processes, and this asymmetry originated from the unidirectional nature of the interfacial exchange coupling. The switching conditions were independent of the magnetic-field cooling conditions below the magnetic field strength of 10 kOe. The analysis of the $E_{\text{th}}-1/H$ relationship suggested that the ME switching was preceded by the antiferromagnetic domain motion. We also found that there was an offset electric field in the $E_{\text{th}}-1/H$ curve, and that it might have originated from the interfacial uncompensated AFM moments in Cr_2O_3 .

ACKNOWLEDGMENTS

This work was partly supported by the JSPS KAKENHI Grant Nos. 16H03832 and 16H02389, the ImPACT program of Council for Science, Technology and Innovation (Cabinet Office, Government of Japan), and the Photonics Advanced Research Center (PARC) at Osaka University.

¹Y.-H. Chu, L. W. Martin, M. B. Holcomb, M. Gajek, S.-J. Han, Q. He, N. Balke, C.-H. Yang, D. Lee, W. Hu, Q. Zhan, P.-L. Yang, A. Fraille-Rodriguez, A. Scholl, S. X. Wang, and R. Ramesh, *Nat. Mater.* **7**, 478 (2008).

- ²X. He, Y. Wang, N. Wu, A. N. Caruso, E. Vescovo, K. D. Belashchenko, P. A. Dowben, and C. Binek, *Nat. Mater.* **9**, 579 (2010).
- ³P. Borisov, A. Hochstrat, X. Chen, W. Kleemann, and C. Binek, *Phys. Rev. Lett.* **94**, 117203 (2005).
- ⁴K. Toyoki, Y. Shiratsuchi, A. Kobane, C. Mitsumata, Y. Kotani, T. Nakamura, and R. Nakatani, *Appl. Phys. Lett.* **106**, 162404 (2015).
- ⁵T. Ashida, M. Oida, N. Shimomura, T. Nozaki, T. Shibata, and M. Sahashi, *Appl. Phys. Lett.* **106**, 132407 (2015).
- ⁶Y. Gao, J.-M. Hu, C. T. Nelson, T. N. Yang, Y. Shen, L. Q. Chen, R. Ramesh, and C. W. Nan, *Sci. Rep.* **6**, 23696 (2016).
- ⁷Y. Shiratsuchi and R. Nakatani, *Mater. Trans.* **57**, 781 (2016).
- ⁸Y. Shiratsuchi, T. Fujita, H. Oikawa, H. Noutomi, and R. Nakatani, *Appl. Phys. Express* **3**, 113001 (2010).
- ⁹W. H. Meiklejohn and C. P. Bean, *Phys. Rev.* **102**, 1413 (1956). 105, 904 (1957).
- ¹⁰J. Nogués and I. K. Schuller, *J. Magn. Magn. Mater.* **192**, 203 (1999).
- ¹¹A. E. Berkowitz and K. Takano, *J. Magn. Magn. Mater.* **200**, 552 (1999).
- ¹²T. Kosub, M. Kopte, R. Hühne, P. Appel, B. Shields, P. Maltinsky, R. Hübner, M. O. Liedke, J. Fassbender, O. G. Schmidt, and D. Makarov, *Nat. Commun.* **8**, 13985 (2017).
- ¹³T. J. Martin and J. C. Anderson, *IEEE Trans. Magn.* **2**, 446 (1966).
- ¹⁴Y. Shiratsuchi, W. Kuroda, T. V. A. Nguyen, Y. Kotani, K. Toyoki, T. Nakamura, M. Suzuki, K. Nakamura, and R. Nakatani, *J. Appl. Phys.* **121**, 073902 (2017).
- ¹⁵A. Iyama and T. Kimura, *Phys. Rev. B* **87**, 180408(R) (2013).
- ¹⁶J. Nogués, T. J. Moran, D. Lederman, and I. K. Schuller, *Phys. Rev. B* **59**, 6984 (1999).
- ¹⁷J. Nogués, D. Lederman, T. J. Moran, and I. K. Schuller, *Phys. Rev. Lett.* **76**, 4624 (1996).
- ¹⁸T. Nozaki, M. Al-Mahwawi, S. P. Pati, S. Ye, and M. Sahashi, *Appl. Phys. Lett.* **110**, 132408 (2017).
- ¹⁹P. Borisov, T. Ashida, T. Nozaki, M. Sahashi, and D. Lederman, *Phys. Rev. B* **93**, 174415 (2016).
- ²⁰L. Fallarino, A. Berger, and C. Binek, *Appl. Phys. Lett.* **104**, 022403 (2014).
- ²¹L. Fallarino, A. Berger, and C. Binek, *Phys. Rev. B* **91**, 054414 (2015).
- ²²Y. Shiratsuchi, T. Nakamura, K. Wakatsu, S. Maenou, H. Oikawa, Y. Narumi, K. Tazoe, C. Mitsumata, T. Kinoshita, H. Nojiri, and R. Nakatani, *Appl. Phys. Lett.* **100**, 262413 (2012).
- ²³V. J. Folen, G. T. Rado, and E. W. Stalder, *Phys. Rev. Lett.* **6**, 607 (1961).
- ²⁴D. N. Astrov, *Sov. Phys. JETP* **11**, 708 (1960).
- ²⁵S. Foner, *Phys. Rev.* **130**, 183 (1963).
- ²⁶Y. Shiratsuchi *et al.*, (to be submitted).
- ²⁷Y. Shiratsuchi, H. Noutomi, H. Oikawa, T. Nakamura, M. Suzuki, T. Fujita, K. Arakawa, Y. Takechi, H. Mori, T. Kinoshira, M. Yamamoto, and R. Nakatani, *Phys. Rev. Lett.* **109**, 077202 (2012).
- ²⁸K. Toyoki, Y. Shiratsuchi, T. Nakamura, C. Mitsumata, S. Harimoto, Y. Takachi, T. Nishimura, H. Nomura, and R. Nakatani, *Appl. Phys. Express* **7**, 114201 (2014).
- ²⁹P. Borisov and W. Kleemann, *J. Appl. Phys.* **110**, 033917 (2011).